


A Pilot Study Evaluating the Use of Dynamic Contrast-Enhanced Perfusion MRI to Predict Local Recurrence After Radiosurgery on Spinal Metastases

Technology in Cancer Research & Treatment
2017, Vol. 16(6) 857–865
© The Author(s) 2017
Reprints and permission:
sagepub.com/journalsPermissions.nav
DOI: 10.1177/1533034617705715
journals.sagepub.com/home/tct


Kiran A. Kumar, MD¹, Kyung K. Peck, PhD^{2,3}, Sasan Karimi, MD², Eric Lis, MD², Andrei I. Holodny, MD², Mark H. Bilsky, MD⁴, and Yoshiya Yamada, MD⁵

Abstract

Purpose: Dynamic contrast-enhanced magnetic resonance imaging offers noninvasive characterization of the vascular microenvironment and hemodynamics. Stereotactic radiosurgery, or stereotactic body radiation therapy, engages a vascular component of the tumor response which may be detectable using dynamic contrast-enhanced magnetic resonance imaging. The purpose of this study is to examine whether dynamic contrast-enhanced magnetic resonance imaging can be used to predict local tumor recurrence in patients with spinal bone metastases who undergo high-dose radiotherapy with stereotactic radiosurgery. **Materials and Methods:** We conducted a study of 30 patients with spinal metastases who underwent dynamic contrast-enhanced magnetic resonance imaging before and after radiotherapy. Twenty patients received single-fraction stereotactic radiosurgery (24 Gy), while 10 received hypofractionated stereotactic radiosurgery (3-5 fractions, 27-30 Gy total). Kaplan-Meier analysis was used to estimate the actuarial local recurrence rates. Two perfusion parameters (K^{trans} : permeability and V_p : plasma volume) were measured for each metastasis. Percentage change in parameter values from pre- to posttreatment was calculated and compared. **Results:** At 20-month median follow-up, 5 of the 30 patients had pathological evidence of local recurrence. One- and 3-year actuarial local recurrence rates were 24% and 44% for the hypofractionated stereotactic radiosurgery cohort versus 5% and 16% for the single-fraction stereotactic radiosurgery cohort ($P = .20$). The average change in V_p and K^{trans} for patients without local recurrence versus those with local recurrence was -76% and -66% versus $+28\%$ and -14% ($P < .01$ for both). With a cutoff point of -20% , V_p had a sensitivity, specificity, positive predictive value, and negative predictive value of 100%, 98%, 91%, and 100%, respectively, for the detection of local recurrence following high-dose radiotherapy. Using this definition, dynamic contrast-enhanced magnetic resonance imaging identified local recurrence up to 18 months (mean [standard deviation], 6.6 [6.8] months) earlier than standard magnetic resonance imaging. **Conclusions:** We demonstrated that changes in perfusion parameters, particularly V_p , after high-dose radiotherapy to spinal bone metastases were predictive of local tumor recurrence. These changes predicted local recurrence on average >6 months earlier than standard imaging did.

Keywords

spine metastases, SBRT, SRS, DCE-MRI, tumor recurrence, high-dose RT

¹ Department of Radiation Oncology, Stanford University, Stanford, CA, USA

² Department of Radiology, Memorial Sloan Kettering Cancer Center, New York, NY, USA

³ Department of Medical Physics, Memorial Sloan Kettering Cancer Center, New York, NY, USA

⁴ Department of Neurosurgery, Memorial Sloan Kettering Cancer Center, New York, NY, USA

⁵ Department of Radiation Oncology, Memorial Sloan Kettering Cancer Center, New York, NY, USA

Corresponding Author:

Yoshiya Yamada, MD, Department of Radiation Oncology, Memorial Sloan Kettering Cancer Center, 1275 York Ave, New York, NY 10065, USA.
Email: yamadaj@mskcc.org



Abbreviations

AUC, area under the curve; AIF, arterial input function; BM, bone marrow; DCE-MRI, dynamic contrast-enhanced magnetic resonance imaging; K^{trans} , permeability; Gd-DTPA, gadolinium diethylene triamine pentaacetic acid; FA, flip angle; FOV, field of view; LC, local control; LR, local recurrence; MRI, magnetic resonance imaging; NPV, negative predictive value; PPV, positive predictive value; ROC, receiver operating characteristic; ROI, region of interest; RT, radiation therapy; SBRT, stereotactic body radiation therapy; SI, signal intensity; SPINO, Spine Response Assessment in Neuro-Oncology; SRS, stereotactic radiosurgery; TR, repetition time; V_p , plasma volume

Received: October 20, 2016; Revised: March 1, 2017; Accepted: March 10, 2017.

Introduction

The spine accounts for up to 70% of all bone metastasis, which is the third most common site of cancer metastasis following lung and liver.^{1,2} Five to ten percent of all patients with cancer develop spinal bone metastases, often causing significant morbidity and mortality.³ Evaluation for the presence of spinal metastases and assessment of treatment response are currently performed using conventional magnetic resonance imaging (MRI).⁴ Images acquired using T1-weighted and short-tau inversion recovery sequences allow for accurate detection of spinal metastases. However, assessment for treatment response is limited and progression is defined as an increase in the size of lesions, but there are no accurate ways of defining a positive treatment response other than the stability of the lesion size.⁵⁻⁹

Dynamic contrast-enhanced MRI (DCE-MRI), as an advanced MR technique, offers noninvasive characterization of vascular microenvironment and hemodynamics that is not available from conventional MRI and the traditional dynamic susceptibility contrast (or T2*) perfusion method.¹⁰ Dynamic contrast-enhanced MRI involves rapid intravenous injection of a contrast agent such as gadolinium diethylene triamine pentaacetic acid (Gd-DTPA), which is measured with a dynamic T1-weighted imaging sequence. The extended Tofts' 2-compartment pharmacokinetic model, which assumes that all contrast is either in the interstitial space or in the intravascular space, is generally used to calculate the intravascular volume, V_p , which is an estimate of tumor vascularity, and the rate of contrast leakage from the intravascular to interstitial space, K^{trans} , which is an estimate of vessel permeability.¹¹⁻¹³ With DCE-MRI, the voxel-wise tracer kinetic analysis during accumulation and distribution of contrast medium in the area of interest offers insight into pathophysiological status of tumor microenvironment. Dynamic contrast-enhanced MRI perfusion parameters have been shown to be able to noninvasively discriminate between hypervascular and hypovascular spinal metastases.^{14,15} Furthermore, DCE-MRI has been used to assess treatment response in patients with spinal metastases treated with high-dose radiation therapy (RT).^{10,16} It has been demonstrated that changes in perfusion parameters, particularly V_p , reflect tumor response to RT in spinal bone metastases.¹⁰

Stereotactic radiosurgery (SRS), or stereotactic body radiation therapy (SBRT), is a technique that allows for the delivery of a single or short course (3-5 treatments) of high-dose RT using conformal techniques with inverse planning. It has been

shown to provide excellent local control (LC; 1-year LC rate >90%) and a low risk of toxicity to spinal cord and other organs at risk in a shorter treatment course than conventional external beam radiation therapy.^{3,17-19} Recent work using experimental mouse tumor models demonstrates that high-dose radiation (>8-10 Gy) induces microvascular endothelial apoptosis in the targeted tissue, in addition to direct tumor cell damage.²⁰ Thus, it is believed that in human tumors as well, SRS engages a vascular component of the tumor response, which may be detectable using DCE-MRI.

In this study, we hypothesize that in addition to evaluating treatment response, changes in DCE-MRI perfusion parameters can be used to predict local tumor recurrence in patients with spinal metastases undergoing high-dose RT.

Materials and Methods

Participants

A waiver of authorization was granted by our institutional review board. We retrospectively examined patients at our institution who received high-dose RT for the treatment of spinal metastasis between 2009 and 2012. Of these, we identified 208 patients who had lesions located between T12 and S5. Lesions outside this area were excluded as DCE-MRI is only routinely performed on the lower part of the spine due to potential image degradation by respiratory and cardiac motion artifacts in the upper spine. We then selected only patients who had at least 1 DCE-MRI scan performed both before and after irradiation, resulting in 48 patients. Finally, we excluded all patients who had scans of poor quality due to prior surgery or kyphoplasty in the area of lesion and ended up with 30 patients in total.

Of the 30 patients in our study, 5 had pathologic evidence of local recurrence (LR), obtained from biopsy during salvage surgery, while 25 were in our LC group. All cases were reviewed by a multidisciplinary team of experts in spinal malignancies consisting of neurosurgeons, radiation and medical oncologists, interventional radiologists, and neuroradiologists. Patients in the LC group showed no radiographic (MRI and Positron Emission Tomography [PET]) evidence of tumor recurrence, defined as a progressive increase in size of the treated lesion with consideration of the clinical scenario, at a median follow-up time of 21 months. For those patients with LR, the median time to proven recurrence, defined as a positive

Table 1. Summary of Patient Characteristics.

	Local Control	Local Recurrence	Total
Number of patients	25 (83%)	5 (17%)	30
Age			
Median (range)	67 (40-89)	56 (52-73)	65 (40-89)
Sex			
Male	15	3	18
Female	10	2	12
Site of spinal metastasis			
T12-L1	8	1	9
L2-L3	10	2	12
L4-L5	7	2	9
Primary neoplasm			
Thyroid	5	0	5
Colon	4	0	4
Breast	3	1	4
Prostate	3	1	4
Renal cell carcinoma	2	2	4
Sarcoma	3	0	3
Lung	2	0	2
Other	3 ^a	1 ^b	4
Treatment regimen			
Single-fraction SRS (24 Gy)	18 (72%)	2 (40%)	20 (67%)
Hypofractionated SRS (27-30 Gy)	7 (28%)	3 (60%)	10 (33%)
Time to recurrence, months			
Median (range)	NA	12 (1-21)	
Follow-up time, months			
Median (range)	21 (5-40)	14 (7-20)	20 (5-40)

Abbreviations: NA, not available; SRS, stereotactic radiosurgery.

^aLiver, esophageal, melanoma.

^bGallbladder.

surgical pathology, was 12 months. The date of detection of LR on standard imaging was based on official radiologist report and review in multidisciplinary tumor board. Twenty of the 30 patients in our cohort received single-fraction (24 Gy) SRS, while 10 of the 30 received hypofractionated (3-5 fractions, 27-30 Gy total) SRS. The use of hypofractionated instead of single-fraction SRS was at the discretion of the treating physician, with primary considerations for hypofractionated SRS including prior radiation to the same lesion or proximity to critical dose-limiting normal structures. The decision Kaplan-Meier analysis was used to estimate the actuarial LR rates of each group, which were compared using a log-rank test. Further patient characteristics, including the site of primary neoplasms, are summarized in Table 1.

Magnetic Resonance Imaging Acquisition

Magnetic resonance imaging scans were acquired with 1.5-T GE scanner (GE Healthcare, Milwaukee, Wisconsin) using an 8-channel cervical-thoracic-lumbar spinal coil. Routine MRI assessments involved the following: sagittal T1 (field of view [FOV], 32-36 cm; slice thickness, 3 mm; repetition time [TR], 400-650 milliseconds; flip angle [FA], 90°) and T2 (FOV,

32-36 cm; slice thickness, 3 mm; TR, 3500-4000 milliseconds; FA, 90°), axial T1 (FOV, 18 cm; slice thickness, 8 mm; FA, 90°) and T2 (FOV, 18 cm; slice thickness, 8 mm; TR, 3000-4000 milliseconds; FA, 90°), and sagittal short inversion time inversion recovery (FOV, 32-36 cm; slice thickness, 3 mm; TR, 3500-6000 milliseconds; FA, 90°).

Dynamic contrast-enhanced MRI of the spine as a part of standard clinical protocol was then acquired. A bolus of Gd-DTPA was administered by a power injector at 0.1 mmol/kg body weight and at a rate of 2 to 3 mL/s. The kinetic enhancement of tissue during and after injection of Gd-DTPA was obtained using a 3-dimensional T1-weighted fast spoiled gradient-echo sequence (TR, 4-5 milliseconds; TE, 1-2 milliseconds; slice thickness, 5 mm; FA, 25°; acquisition matrix, 256 × 128, FOV, 32 cm; total 40 dynamic phases; temporal resolution [Δt] of 5 seconds) and consisted of 10 to 12 images in sagittal plane. First 10 phases were acquired without contrast injection and have been used to calculate T1. Sagittal and axial T1-weighted post-Gd-DTPA MR images were acquired after DCE-MRI.

Data Analysis

Dynamic image processing software (NordicICE: version 2.3; NordicNeuroLab [NNL], Bergen, Norway) was used for data processing. Preprocessing steps included background noise removal, spatial and temporal filtering, and automatic detection of arterial input function (AIF) from the aorta. The AIF was individually measured in each acquisition of every patient. Pixels with a large change in signal intensity (SI), with a rapid change immediately after bolus injection, and with an early peak in intensity in the image(s) have been chosen for AIF. Linear assumption was made between change in SI and gadolinium concentration to convert SI curve to concentration-time curve. At low concentrations (below about 10 mM), the linearity assumption holds because the relationship between SI and Gd concentration is approximately linear.²¹ The extended Tofts' 2-compartment pharmacokinetic model was applied for calculation of parameters V_p and K^{trans} , in which V_p = intravascular plasma volume and K^{trans} (permeability) = rate constant of Gd leakage from intravascular to interstitial space.¹¹

The K^{trans} and V_p maps were obtained for each patient in a region of interest (ROI) within the tumor. On each map, ROIs were drawn freehand by the same investigator around regions of increased SI in tumor area, defining regions of higher overall perfusion. If tumor was present on multiple slices, the slice containing the most enhancing voxels (SliceMax) was used.²² Regions of interest were also drawn over normal unirradiated bone marrow (BM) 2 to 3 vertebrae away from the ROI, which was used as a baseline to measure relative SI of each lesion. Regions of interest around metastatic lesions were placed in the solid part of the tumor with careful consideration to avoid venous structures, hemangiomas, disc spaces, cortical bone, and spondylotic changes. Anatomical images that overlaid onto the DCE-MRI perfusion images were used in ROI placements. Relative SI values were obtained for each lesion before and

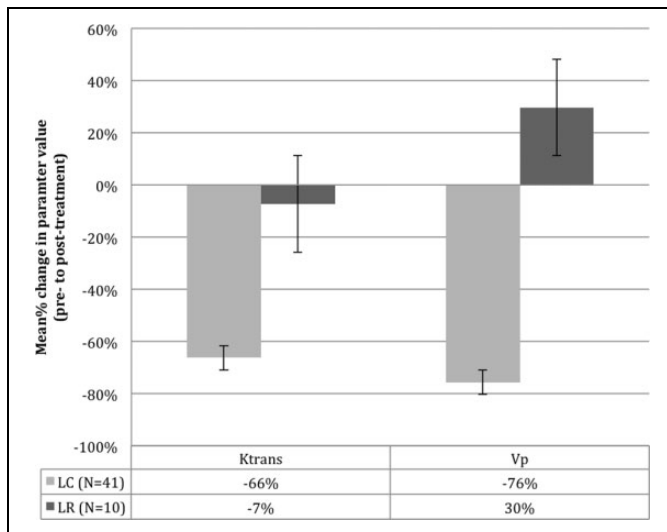


Figure 1. Average percentage change in perfusion parameters from pre- to posttreatment scans. Both permeability (K^{trans}) and plasma volume (V_p) showed a significant difference between scans from the local control and local recurrence groups ($P < 0.01$ for both). Standard error bars are shown.

after radiotherapy and were compared in terms of percentage change, calculated as: $([\text{Pre} - \text{Post}]/\text{Pre}) \times 100$. The mean percentage change in perfusion parameters (V_p and K^{trans}) from pre- to posttreatment scans was calculated in each group (LR and LC).

Statistical Analysis

A Mann-Whitney U test, at a significance level of $P \leq .01$, was performed to quantify and compare the significance of the perfusion parameters (K^{trans} and V_p) in both groups. To assess perfusion parameters as predictors of LR, receiver operating characteristic (ROC) curves were drawn for both V_p and K^{trans} using the pROC package in R version 3.1.0. These curves were used to determine the ideal cutoff value that provides the maximum sensitivity and specificity for each parameter. Area under the curve (AUC) was also calculated for each to compare the 2 parameters. Sensitivity, specificity, positive predictive value (PPV), and negative predictive value (NPV) at the ideal cutoff value for each parameter were calculated using this software. Relationship between time after radiation treatment and

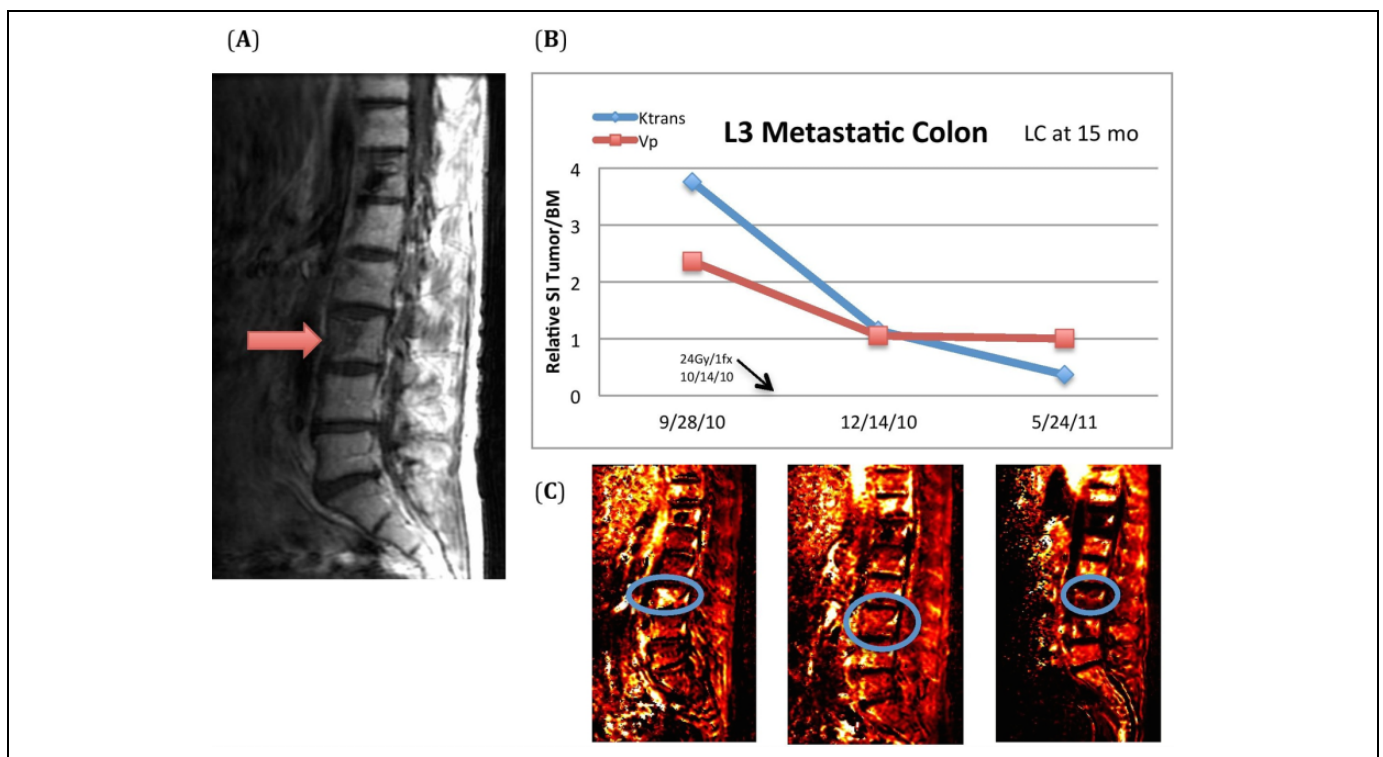


Figure 2. Example of a case in the local control group. This patient had a colon adenocarcinoma metastasis to the spine. A, Sagittal T1-weighted image showing a metastatic lesion at the L3 vertebra. B, Graph displaying relative signal intensity (SI) of the tumor to adjacent normal bone marrow (BM) from plasma volume (V_p) and permeability (K^{trans}) perfusion maps at 3 different time points: on September 28, 2010, before irradiation (in this case, 24 Gy in a single fraction), and twice after irradiation, on December 14, 2010 and May 24, 2011. The relative SI of the tumor for both V_p and K^{trans} is several times that of the normal BM prior to irradiation but becomes similar to or less than the SI of the normal BM after irradiation. C, The V_p perfusion maps are shown for the same 3 time points as in the line graph. Qualitatively, it is obvious that prior to treatment (left), the tumor has a greater SI than adjacent normal BM, but after treatment (middle and right), the SI becomes equal to or less than the adjacent normal BM.

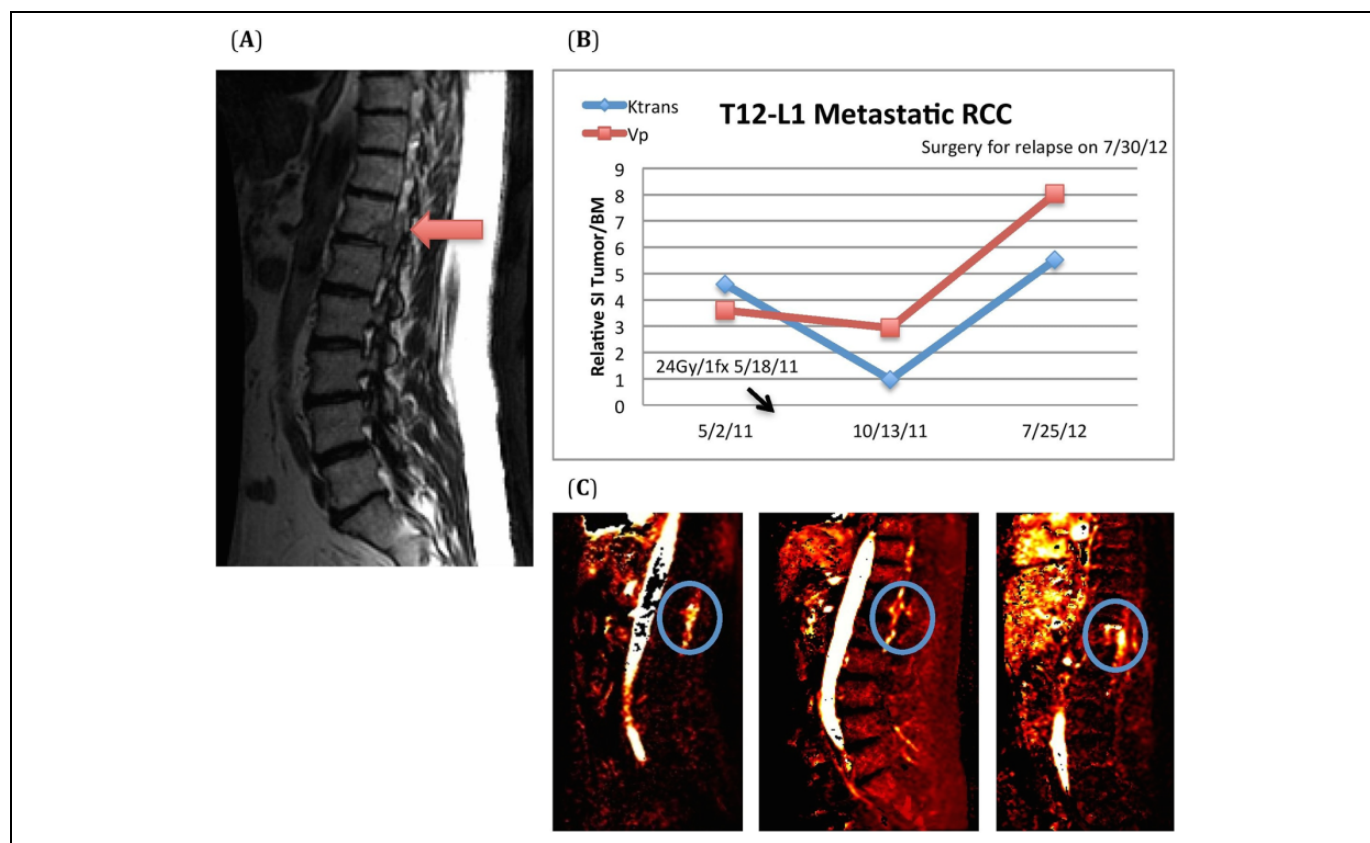


Figure 3. Example of a case in the local recurrence group. This patient had a renal cell carcinoma metastasis to the spine. A, Sagittal T1-weighted image showing a metastatic lesion at T12-L1. B, Graph displaying relative signal intensity (SI) of the tumor to the adjacent normal bone marrow (BM) from plasma volume (V_p) and permeability (K^{trans}) perfusion maps at 3 different time points: on May 2, 2011, before irradiation (in this case, 24 Gy in a single fraction), and twice after irradiation, on October 13, 2011 and July 25, 2012. The relative SI tumor/BM is high prior to irradiation, but unlike with the tumor control example (Figure 2), it stays high after irradiation and eventually increases even more. C, The V_p perfusion maps are shown for the same 3 time points as in the line graph. Qualitatively, it is evident that both prior to irradiation (left) and after (middle), the tumor has a greater SI than the adjacent normal BM, and with additional time (right), the tumor SI increases even further.

percentage change in V_p in either group (LC and/or LR) has been assessed using ordinary least squares regression.

Results

Of the 20 patients who received single-fraction SRS, only 2 (10%) had LR, while 3 (30%) of 10 patients who received hypofractionated SRS had LR. The 1- and 3-year actuarial LR rates were 5% and 16% for single-fraction SRS group versus 24% and 44% for hypofractionated SRS group ($P = .20$).

The mean percentage changes in V_p and K^{trans} from pre- to posttreatment scans were both significantly different between the LC and LR groups (Figure 1). The mean percentage changes in K^{trans} for LC and LR groups were -66% and -7% , respectively ($P < .01$). The mean percentage changes in V_p for LC and LR groups were -76% and $+30\%$, respectively ($P < .01$).

Sample cases in the LC (Figure 2) and LR groups (Figure 3) are shown. For each patient, a sagittal T1-weighted image was used to identify metastatic lesion (Figures 2A and 3A). The V_p

and K^{trans} perfusion maps were then generated as described above and used to both quantitatively calculate relative SI of the tumor/BM (Figures 2B and 3B) and qualitatively assess tumor perfusion (Figures 2C and 3C). In addition to quantitative difference in percentage change of V_p and K^{trans} between the LC and LR groups, qualitatively it is obvious whether the patient has tumor control versus tumor recurrence (Figures 2C vs 3C).

To assess the performance of perfusion parameters in predicting tumor recurrence, ROC curves were drawn for both K^{trans} and V_p (Figure 4). The AUC was 0.866 for K^{trans} and 0.998 for V_p . The sensitivity and the specificity for predicting LR for change in K^{trans} with a cutoff value of -50% were 80% and 76%, respectively. This parameter had a PPV of 44% and an NPV of 94%. The sensitivity and the specificity for predicting LR for change in V_p with a cutoff value of -20% were 100% and 98%, respectively. This parameter had a PPV of 91% and an NPV of 100%.

Details of each recurrence case, including primary tumor type and location, average change in perfusion parameters, and

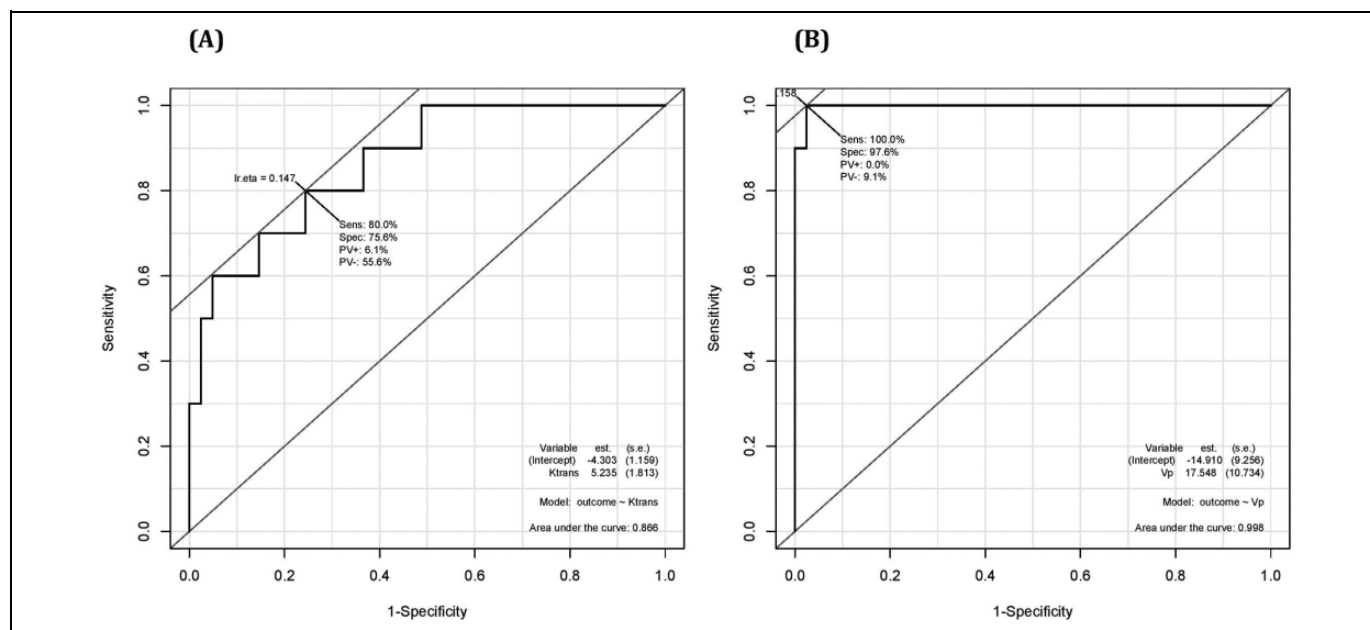


Figure 4. Receiver operating characteristic (ROC) curves examining perfusion parameters permeability (K^{trans} ; A) and plasma volume (V_p ; B) for the detection of local recurrence of spinal metastasis after irradiation. The area under the ROC curve was 0.866 for K^{trans} and 0.998 for V_p . For K^{trans} (A), the optimal cutoff point for the detection of LR was -50% , resulting in a sensitivity of 80% and a specificity of 76%. For V_p (B), the optimal cutoff point for the detection of LR was -20% , resulting in a sensitivity of 100% and a specificity of 98%.

Table 2. Recurrence Cases.

Recurrence No.	Primary Tumor/Location	Months to First Posttreatment Scan	Average % Change in K^{trans}	Average % Change in V_p	No. Months Changes in V_p Predicted LR Before Standard Imaging
1	RCC/T12-L1	2	-10	+15	4
2	Cholangiocarcinoma/L4	14	-10	0	4
3	RCC/L4	1	+23	+17	0 ^a
4	Prostate/L2	5	+78	+67	7
5	Breast/L2	2	-42	+7	18

Abbreviations: K^{trans} , permeability; RCC, Renal Cell Carcinoma; V_p , plasma volume.

^aLocal recurrence (LR) was detected on standard imaging at the same time as dynamic contrast-enhanced magnetic resonance imaging (DCE-MRI).

time until first posttreatment scan are displayed in Table 2. Additionally, the table shows the time interval between first detection of the LR by perfusion parameters (V_p with a cutoff of -20%) versus standard imaging for each case. DCE-MRI identified LR up to 18 months (mean [standard deviation], 6.6[6.8] months) earlier than standard MRI.

Discussion

Recent studies have demonstrated that DCE-MRI can detect tumor response to high-dose RT in spinal bone metastases through changes in perfusion parameters shortly after treatment.^{10,16} Here, we show that in addition to evaluating tumor response to treatment, DCE-MRI can predict local tumor recurrence following high-dose RT. Specifically, average change in perfusion parameters V_p and K^{trans} differed significantly from the LC group compared with the LR group ($P < .01$). A more

significant difference was seen with V_p , which had an average change of -76% in the LC group versus $+30\%$ in the LR group. With a cutoff point of -20% , V_p had a sensitivity of 100% and a specificity of 98% for the detection of LR following high-dose RT. Using this definition, DCE-MRI was able to predict local tumor recurrence on average 6.6 months earlier than it was detected using standard imaging.

Multiple studies have examined the use of DCE-MRI in assessing radiation treatment response in a variety of sites, including the brain, head and neck, breast, cervix, and prostate.²³⁻²⁷ Furthermore, some studies have shown that DCE-MRI may be able to distinguish tumor recurrence from treatment change, for example, in patients with gliomas.^{25,28} However, it was not until recently that DCE-MRI was used to assess radiation treatment response in the spine. In a heterogeneous cohort of 19 spinal bone metastases treated with RT, Chu *et al* reported that changes in V_p most strongly predicted

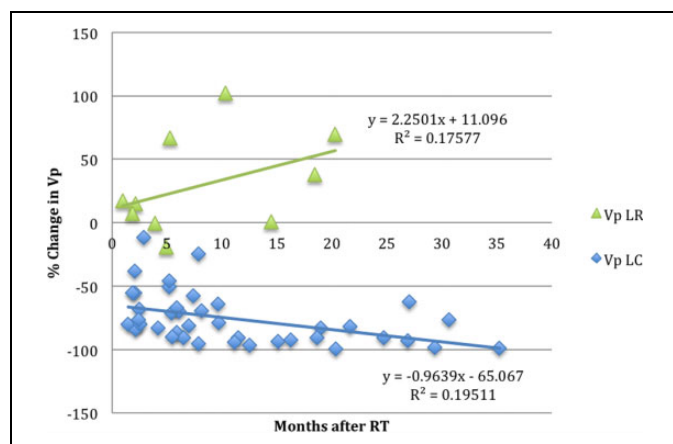


Figure 5. Diagram showing the relationship between time after irradiation and percentage change in plasma volume (V_p). The green triangles are data points from the local recurrence (LR) group, while the blue diamonds are data points from the local control (LC) group. The linear curve for each group was obtained using ordinary least squares regression. The slope coefficients for the LR and LC groups were 2.25 and -0.96 , respectively; both did not differ significantly from 0 ($P > .05$).

treatment response, with all successfully treated lesions showing decreases in V_p , but the 2 treatment failures showing dramatic increases in V_p .¹⁰ Spratt *et al* reported that in a homogenous cohort of 12 metastatic sarcoma lesions to the spine treated with SBRT, with 1 local failure, a combination of changes in perfusions parameters (K^{trans} , V_p) had 100% accuracy in predicting LC better than conventional size and subjective neuroradiology impressions.¹⁶ Our study builds upon these as it demonstrates that in a larger cohort of spinal bone metastases treated with high-dose RT, including 5 pathologically proven local tumor recurrences, DCE-MRI perfusion parameters can be used not only to evaluate treatment response shortly after RT but also to predict local tumor recurrence in the future.

While both V_p and K^{trans} were found to be predictive of LR, V_p was much more accurate, as evident by the higher AUC. This is congruent with previous results that showed V_p to be more reflective of tumor response to RT in BM than K^{trans} .¹⁰ The V_p decreases in successfully treated lesions likely because RT causes a decrease in vascularity. Conversely, the increased V_p in cases of LR is perhaps due to increased angiogenesis in recurrent bone metastases.² K^{trans} , an estimate of the velocity of blood transfer from the vascular compartment to the interstitial space, has previously been used to assess tumor vascular properties in the brain and other soft tissues but may not be as reliable in BM due to physiologic differences between brain and bone tissue.¹¹

Our analysis assumed that the time following treatment does not affect change in perfusion parameters. While this seems likely with locally controlled tumors, it is less clear with tumors that recur. Comparing time after radiation to percentage change in V_p showed no correlation in the LC group but a trend toward a significantly positive correlation in the LR group (Figure 5).

This suggests a possible relationship between time and increase in perfusion parameters for tumors that locally recur, which would be expected as tumors continue to grow over time. It also raises the following question: at what point following treatment, using our cutoff of -20% for V_p , can LR be detected? The earliest posttreatment scan available in our LR group was 1 month, which did predict LR; thus, it may be possible to predict LR at this early time interval and perhaps even earlier.

Our results have significant clinical implications. Early detection of treated tumors that are likely to recur would allow for more timely interventions and likely improved outcomes. Similarly, knowing early on that a tumor was treated successfully and is unlikely to locally recur could decrease patient stress and cost of additional surveillance tests and imaging. The Spine Response Assessment in Neuro-Oncology (SPINO) group has published its preliminary recommendations for imaging-based local tumor response after spine SBRT, as Response Evaluation Criteria in Solid Tumors have been shown to be inadequate in this setting. We believe that in the future, with further evaluation and validation prospectively, changes in DCE-MRI perfusion parameters can be integrated into the SPINO criteria to better define local progression after spine SBRT.

This study is not without its limitations. The sample size is small and heterogeneous in terms of primary tumor histology and treatments, in part due to a requirement of both pre- and posttreatment DCE-MRI scans and limited availability. We acknowledge that the effect of different fractionation schemes and systemic therapies on DCE-MRI is unknown and a potential confounder. However, the differences in perfusion parameters were dramatic enough between the groups (LC vs LR) that ROC analysis could be performed and the predictive value of the parameters was found to be very good, especially V_p . Another limitation is that this was a retrospective study. Because of this, the timing before and after treatment of DCE-MRI scans was not consistent among patients. Despite the variation in timing, we were still able to show significant differences between the LC and LR groups. There are also several technical challenges. To apply a pharmacokinetic model for quantitative analysis, both the precontrast T1 value and AIF must be accurately measured. In the design of DCE-MRI studies, competing demands for high spatial resolution, coverage, and signal-to-noise ratio often result in inadequate temporal resolution for reliable measurement of the AIF. Saturation effects and mis-sampling can affect the AIF time course and initial contrast bolus, and dispersion of the AIF before it reaches the ROI can also affect DCE-MRI quantification. Furthermore, due to concern about potential image degradation by respiratory and cardiac motion artifacts, we limited our study to metastases of the lumbosacral spine only.

Future studies should include upper spinal bone metastases if DCE-MRI is to be considered widely for response assessment after high-dose RT to the spine. Additionally, a prospective study is needed to answer questions regarding timing to

change in perfusion parameters and if results vary based on primary histology. Finally, a direct comparison to standard imaging prospectively could more accurately determine the benefit of DCE-MRI in terms of earlier local tumor recurrence detection.

Conclusion

Dynamic contrast-enhanced MRI can noninvasively detect early treatment response and predict local tumor recurrence in spinal bone metastases treated with high-dose RT. This has important clinical implications that may ultimately lead to improved patient care.

Authors' Note

Portions of this work were presented as an oral presentation in the 99th Scientific Assembly and Annual meeting in the Radiological Society of North America (RSNA) on December 2, 2013.

Acknowledgments

The authors would like to acknowledge Ashwin Kotwal, MD, for helping with statistical analysis and Rupali Kumar, MD, for helping use the R statistical software to generate receiver operating characteristic (ROC) curves. The authors would like to acknowledge the Radiology Development Fund.

Declaration of Conflicting Interests

The author(s) declared the following potential conflicts of interest with respect to the research, authorship, and/or publication of this article: Dr Yamada reports being a consultant for Varian Medical Systems and member of the speaker bureau of the Institute for Medical Education.

Funding

The author(s) disclosed receipt of the following financial support for the research, authorship, and/or publication of this article: Funding from the Department of Radiology at Memorial Sloan Kettering Cancer Center.

References

- Chao ST, Koyfman SA, Woody N, et al. Recursive partitioning analysis index is predictive for overall survival in patients undergoing spine stereotactic body radiation therapy for spinal metastases. *Int J Radiat Oncol Biol Phys*. 2012;82(5):1738-1743.
- Togawa D, Lewandrowski KU. The pathophysiology of spinal metastases. In: McLain R, Lewandrowski KU, Markman M, et al, eds. *Current Clinical Oncology: Cancer in the Spine: Comprehensive Care*. Totowa, NJ: Humana Press, Inc; 2006:17-23.
- Gerszten PC, Mendel E, Yamada Y. Radiotherapy and radiosurgery for metastatic spine disease: what are the options, indications, and outcomes? *Spine*. 2009;34(suppl 22):S78-S92.
- Traill Z, Richards MA, Moore NR. Magnetic resonance imaging of metastatic bone disease. *Clin Orthop Relat Res*. 1995;(312):76-88.
- Biffar A, Dietrich O, Sourbron S, Duerr HR, Reisder MR, Baur-Melnyk A. Diffusion and perfusion imaging of bone marrow. *Eur J Radiol*. 2010;76(3):323-328.
- Yankelevitz DF, Henschke CI, Knapp PH, Nisce L, Yi Y, Cahill P. Effect of radiation therapy on thoracic and lumbar bone marrow: evaluation with MR imaging. *AJR Am J Roentgenol*. 1991;157(1):87-92.
- Otake S, Mayr NA, Ueda T, Magnotta VA, Yuh WT. Radiation-induced changes in MR signal intensity and contrast enhancement of lumbosacral vertebrae: do changes occur only inside the radiation therapy field? *Radiology*. 2002;222(1):179-183.
- Koo KH, Dussault R, Kaplan P, et al. Age-related marrow conversion in the proximal metaphysis of the femur: evaluation with T1-weighted MR imaging. *Radiology*. 1998;206(3):745-748.
- Vande Berg BC, Malghem J, Lecouvet FE, Maldague B. Magnetic resonance imaging of the normal bone marrow. *Eur Radiol*. 1998;8(8):1327-1334.
- Chu S, Karimi S, Peck KK, et al. Measurement of blood perfusion in spinal metastases with dynamic contrast-enhanced magnetic resonance imaging. *Spine*. 2013;38(22):E1418-E1424.
- Tofts PS, Brix G, Buckley DL, et al. Estimating kinetic parameters from dynamic contrast-enhanced T1-weighted MRI of a diffusible tracer: standardized quantities and symbols. *J Magn Reson Imaging*. 1999;10(3):223-232.
- Dyke JP, Aaron RK. Noninvasive methods of measuring bone blood perfusion. *Ann N Y Acad Sci*. 2010;1192:95-102.
- Hylton N. Dynamic contrast-enhanced magnetic resonance imaging as an imaging biomarker. *J Clin Oncol*. 2006;24(20):3293-3298.
- Saha A, Peck KK, Lis E, Holodny AI, Yamada Y, Karimi S. Magnetic resonance perfusion characteristics of hypervascular renal and hypovascular prostate spinal metastases: clinical utilities and implications. *Spine*. 2014;39(24):E1433-E1440.
- Khadem NR, Karimi S, Peck KK, et al. Characterizing hypervascular and hypovascular metastases and normal bone marrow of the spine using dynamic contrast-enhanced MR imaging. *Am J Neuroradiol*. 2012;33(11):2178-2185.
- Spratt DE, Arevalo-Perez J, Leeman JE, et al. Early magnetic resonance imaging biomarkers to predict local control after high-dose stereotactic body radiotherapy for patients with sarcoma spine metastases. *Spine J*. 2016;16(3):291-298.
- Bilsky MH, Gerszten P, Laufer I, Yamada Y. Radiation for primary spine tumors. *Neurosurg Clin N Am*. 2008;19(1):119-123.
- Yamada Y, Bilsky MH, Lovelock DM, et al. High-dose, single-fraction image-guided intensity-modulated radiotherapy for metastatic spinal lesions. *Int J Radiat Oncol Biol Phys*. 2008;71(2):484-490.
- Moulding HD, Elder JB, Lis E, et al. Local disease control after decompressive surgery and adjuvant high-dose single-fraction radiosurgery for spine metastases. *J Neurosurg Spine*. 2010;13(1):87-93.
- Garcia-Barros M, Paris F, Cordon-Cardo C, et al. Tumor response to radiotherapy regulated by endothelial cell apoptosis. *Science*. 2003;300(5622):1155-1159.
- Biglands JD, Radjenovic A, Ridgway JP. Cardiovascular magnetic resonance physics for clinicians: part II. *J Cardiovasc Magn Reson*. 2012;14:66.

22. Craciunescu O, Yoo DS, Cleland E, et al. Dynamic contrast-enhanced MRI in head-and-neck cancer: the impact of region of interest selection on the intra- and interpatient variability of pharmacokinetic parameters. *Int J Radiat Oncol Biol Phys.* 2012; 82(3):e345-e350.
23. Akin O, Gultekin DH, Vargas HA, et al. Incremental value of diffusion weighted and dynamic contrast enhanced MRI in the detection of locally recurrent prostate cancer after radiation treatment: preliminary results. *Eur Radiol.* 2011;21(9): 1970-1978.
24. Kim J, Kim CK, Park BK, Park SY, Huh SJ, Kim B. Dynamic contrast-enhanced 3-T MR imaging in cervical cancer before and after concurrent chemoradiotherapy. *Eur Radiol.* 2012;22(11): 2533-2539.
25. Shin KE, Ahn KJ, Choi HS, et al. DCE and DSC MR perfusion imaging in the differentiation of recurrent tumour from treatment-related changes in patients with glioma. *Clin Radiol.* 2014;69(6): e264-e272.
26. Wang CH, Yin FF, Horton J, Chang Z. Review of treatment assessment using DCE-MRI in breast cancer radiation therapy. *World J Methodol.* 2012;4(2):46-58.
27. Zheng D, Chen Y, Liu X, et al. Early response to chemoradiotherapy for nasopharyngeal carcinoma treatment: value of dynamic contrast-enhanced 3.0 T MRI. *J Magn Reson Imaging.* 2015; 41(6):1528-1540.
28. Larsen VA, Simonsen HJ, Law I, Larsson HB, Hansen AE. Evaluation of dynamic contrast-enhanced T1-weighted perfusion MRI in the differentiation of tumor recurrence from radiation necrosis. *Neuroradiology.* 2013;55(3):361-369.